

# Synthesis and Structure of *cis*-Palladium(II) Carbene Complexes Containing the 1,3-Diallylimidazolidin-2-ylidene Ligand: *trans* → *cis* Rearrangement

José A. Chamizo,<sup>†</sup> Jorge Morgado,<sup>\*,‡</sup> Miguel Castro,<sup>†</sup> and Sylvain Bernès<sup>†,§</sup>

Programa de Ingeniería Molecular, Instituto Mexicano del Petróleo, Eje Central Lázaro Cárdenas, C.P. 07730 México D.F., México, and Facultad de Química, Universidad Nacional Autónoma de México, Ciudad Universitaria, C.P. 04510 México D.F., México

Received March 14, 2002

Palladium(II) carbene complexes with a 1,3-diallylimidazolidin-2-ylidene ligand ( $L^{\text{Allyl}}$ ) were prepared and characterized by IR, NMR, and mass spectra. The *trans* → *cis* rearrangement of the *trans*-[PdCl<sub>2</sub>( $L^{\text{Allyl}}$ )<sub>2</sub>] complex was observed. The relative thermodynamic stability of these isomers was studied using DFT calculations.

## Introduction

Research on the synthesis, reactivity, and structural characterization of metal carbene complexes has led to the development of a major area of organometallic chemistry, due, primarily, to the numerous catalytic and stoichiometric reactions in which these species are often involved.<sup>1,2</sup> A vast majority of these types of compounds contain at least one heteroatom attached to the carbene carbon atom and are the so-called Fischer-type carbene complexes. One of the preparative methods available for these types of complexes is to treat electron-rich olefin ( $L^{\text{R}_2}$ )<sup>3</sup> with several metal complexes.<sup>4</sup> However, attempts to prepare the electron-rich olefin N-allyl-functionalized ( $L^{\text{Allyl}_2}$ ) has been unsuccessful.<sup>5</sup> During our ongoing investigations of imidazoline carbene chemistry we have isolated and structurally characterized carbene complexes in which  $L^{\text{Allyl}}$  is the ligand, which are accessible by in situ preparation.<sup>6,7</sup> In addition, we have recently reported the preparation of *trans*-bis(carbene) nickel(II) and palladium(II) complexes prepared from the amination **1** in high yield<sup>8</sup> (e.g., **4**, Scheme 1). This bis(carbene) complex has proved to be particularly interesting since it presents strong evidence for *trans* → *cis* isomerization. The *cis*–*trans* isomerization of

[PdR<sub>2</sub>L<sub>2</sub>] complexes is a very important reaction in organopalladium(II) chemistry.<sup>9</sup> We now wish to report that we have successfully achieved the synthesis of four *cis*-palladium(II) carbene complexes. On the other hand, the *cis*-bis(carbene) isomer is formed at room temperature in high yield from the direct rearrangement of the pure *trans*-bis(carbene) complex.

## Results and Discussion

The successive treatment of [PdCl<sub>2</sub>(PEt<sub>3</sub>)<sub>2</sub>] with the amination **1** leads to the formation of *trans*-mono- and *trans*-bis(carbene) complexes in high yield.<sup>8</sup> If, on the other hand, [Pd<sub>2</sub>Cl<sub>4</sub>(PEt<sub>3</sub>)<sub>2</sub>] is employed, the *cis*-complex **2** is obtained in high yield as the only organometallic product (Scheme 1) on the basis of spectroscopic data and a single-crystal X-ray diffraction study (Table 1 and Figure 1, vide infra). The chloride ligands of *cis*-[PdCl<sub>2</sub>( $L^{\text{Allyl}}$ )PEt<sub>3</sub>] are readily substituted by Br<sup>−</sup> and I<sup>−</sup> ligands to produce complexes **5** and **6**, respectively. The infrared spectra of **2**, **5**, and **6** exhibit characteristic absorptions due to the  $L^{\text{Allyl}}$  ligand and two bands in the metal–halogen region, which suggest a *cis* coordination geometry. The mass spectra of the complexes are in agreement with their formulation as palladium dihalide derivatives, showing consecutive peaks corresponding to  $m/z = [M^+ - X]$  and  $[M^+ - 2X]$ . The carbon and proton resonances of these complexes are very similar; CH<sub>2</sub> protons of the imidazolidine ring were observed as a doublet (at about  $\delta = 3.6$  ppm) for all the *cis*-isomers and the characteristic signal pattern of the methyl protons in the phosphine ligand was observed.

Figure 1 shows a square plane defined around the palladium atom for complex **2**. The carbene carbon atom is approximately trigonal, and the N–C–(Pd)–N plane lies at 92.3° to the coordination plane of the palladium (PdCCl<sub>2</sub>P). The Pd–C bond length (1.972(4) Å) is somewhat shorter than an ordinary Pd–C single bond length; the Pd–C(sp<sup>2</sup>) distances of metal– $\sigma$ -vinyl bonds

\* To whom all correspondence should be addressed. Instituto Mexicano del Petróleo. E-mail: jmorgado@imp.mx.

<sup>†</sup> Universidad Nacional Autónoma de México. E-mail: jchamizo@servidor.unam.mx and castro@quetzal.pquim.unam.mx.

<sup>‡</sup> Instituto Mexicano del Petróleo.

<sup>§</sup> Present address: Centro de Química, Instituto de Ciencias, BUAP, México.

(1) Schubert, U., Ed. *Advances in Metal Carbene Chemistry*; Kluwer Academic Publishers: The Netherlands, 1989.

(2) Dötz, K. H. *Transition Metal Carbene Complexes*; Verlag Chemie: Weinheim, 1983.

(3) 1',3,3'-Tetrasubstituted-2,2'-bi-imidazolidinylidene ( $L^{\text{R}_2}$ ).

(4) Lappert, M. F. *J. Organomet. Chem.* **1975**, *100*, 139. Lappert, M. F. *J. Organomet. Chem.* **1988**, *358*, 185.

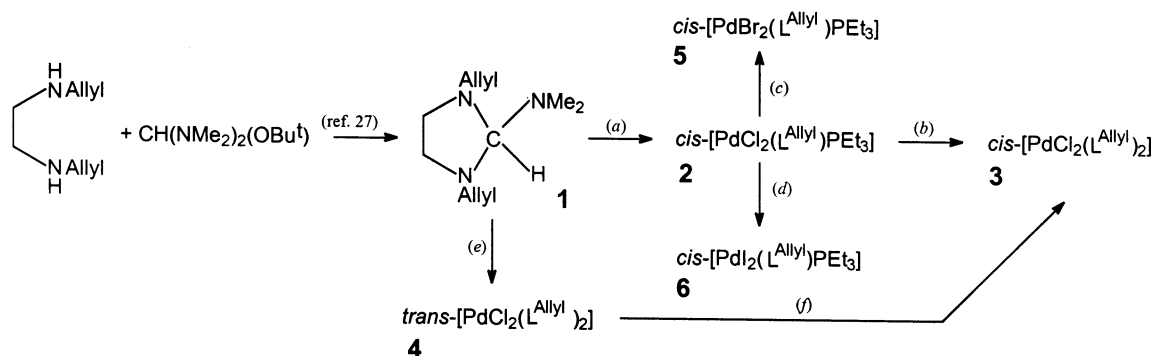
(5) Chamizo, J. A.; Lappert, M. F. *J. Org. Chem.* **1989**, *54*, 4684.

(6) Chamizo, J. A.; Hitchcock, P. B.; Jasim, H. A.; Lappert, M. F. *J. Organomet. Chem.* **1993**, *451*, 89.

(7) Chamizo, J. A.; Morgado, J.; Álvarez, C.; Toscano, R. A. *Transition Met. Chem.* **1995**, *20*, 508.

(8) Chamizo, J. A.; Morgado, J.; Bernès, S. *Transition Met. Chem.* **2000**, *25*, 161.

(9) Cross, R. J. *Adv. Inorg. Chem.* **1989**, *34*, 219.

Scheme 1<sup>a</sup>

<sup>a</sup> Reactions and conditions. All reactions in benzene at room temperature: (a)  $\text{Pd}_2\text{Cl}_4(\text{PET}_3)_2$ , (b) a)minal  $[\text{C}_3\text{H}_5\text{NCH}_2\text{CH}_2(\text{C}_3\text{H}_5)\text{NC}(\text{NMe}_2)\text{H}]$ , **1**, (c) LiBr, acetone, (d) NaI, acetone, (e)  $\text{trans-}[\text{PdCl}_2(\text{L}^{\text{Allyl}})\text{PEt}_3]$ , **4**, (f) stirring 48 h.

Table 1. Experimental Crystallographic Data for **2** and **3**

	<b>2</b>	<b>3</b>
formula	$\text{C}_{15}\text{H}_{29}\text{Cl}_2\text{N}_2\text{PPd}$	$(\text{C}_9\text{H}_{14}\text{N}_2)_2\text{Pd}\cdot(\text{H}_2\text{O})_{2.5}$
space group	$Pca2_1$	$P2_1/c$
<i>b</i> (Å)	7.8117(12)	18.080(4)
<i>c</i> (Å)	17.865(3)	13.9517(19)
$\beta$ (deg)		104.594(12)
<i>V</i> (Å <sup>3</sup> )	1993.3(5)	2439.4(8)
<i>Z</i>	4	4
temperature (K)	298	298
$2\theta$ range (deg)	4.56–60.00	3.76–48.00
no. of data collected	3814	4875
no. of unique data	3148 (1.95%)	3817 (9.00%)
$R_{\text{int}}$		
goodness-of-fit	1.060	1.008
$R_1^a$ (obsd data)	0.0284	0.082
$wR_2^b$ (all data)	0.0725	0.2518

<sup>a</sup>  $R_1 = \sum ||F_o| - |F_c|| / \sum |F_o|$ . <sup>b</sup>  $wR_2 = [\sum w(F_o^2 - F_c^2)^2 / \sum w(F_o^2)]^{1/2}$ .

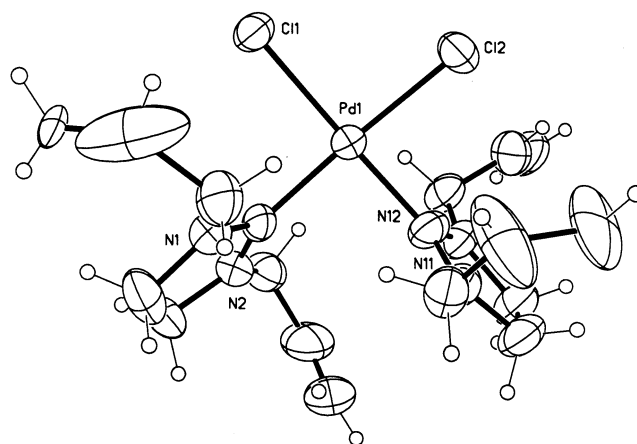


Figure 2. Molecular structure of  $\text{cis-}[\text{PdCl}_2(\text{L}^{\text{Allyl}})_2]$  **3**. Thermal ellipsoids are at the 30% probability level. Water molecules are omitted for clarity.

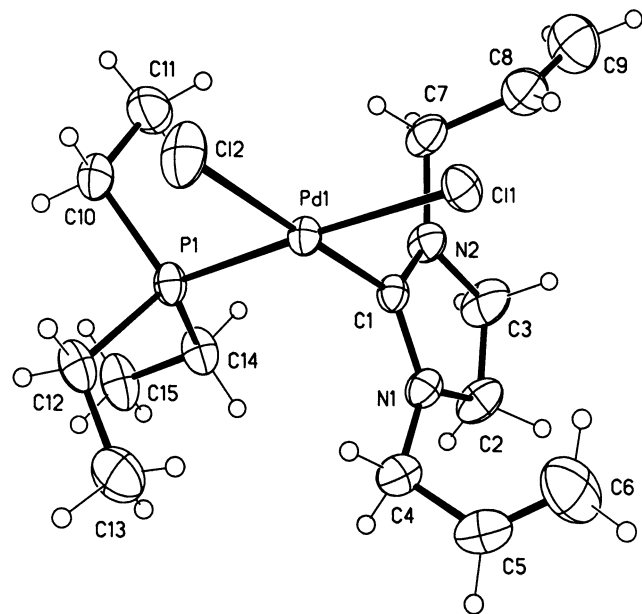


Figure 1. Molecular structure of  $\text{cis-}[\text{PdCl}_2(\text{L}^{\text{Allyl}})\text{PEt}_3]$  **2**. Thermal ellipsoids are at the 30% probability level.

in  $\text{cis-bis}[1,2\text{-bis}(\text{trifluoromethyl})\text{-3-acetyl-4-oxopent-1-enyl-}O,C]\text{palladium(II)}$  are 1.993 Å.<sup>10</sup> The Pd–P distance enables us to estimate the *trans* influence of the

carbene ligand, which is approximately equal to that of a tertiary phosphine, as has been found (based on the Pd–C bond length) for the carbene ligand  $\text{L}^{\text{Ph}}$  in  $\text{cis-}[\text{PtCl}_2(\text{L}^{\text{Ph}})\text{PEt}_3]$ .<sup>11</sup>

We have also prepared and structurally characterized (Table 1 and Figure 2) the *cis*-bis(carbene) complex  $[\text{PdCl}_2(\text{L}^{\text{Allyl}})_2]$  **3**. This complex may be prepared by two different methods, one strategic (b) and the other unexpected (f); see Scheme 1. Both methods provide **3** in high yield. Surprisingly, however, a *trans* → *cis* isomerization was observed in the second case and deserves a comment. The <sup>1</sup>H NMR spectrum of **4** shows characteristic resonances for the allyl group and a singlet for the imidazolidine ring protons, and a resonance for the carbene carbon atoms is observed at 199.0 ppm in the <sup>13</sup>C NMR spectrum. When a light yellow solution of  $\text{trans-}[\text{PdCl}_2(\text{L}^{\text{Allyl}})_2]$  **4** (the configuration was confirmed by spectroscopic and X-ray analysis)<sup>8</sup> in benzene was stirred at room temperature, the color was discharged. The <sup>13</sup>C NMR spectrum shows two resonances for the quaternary carbon atoms at 190.4 (major signal, *cis*-isomer) and 199.0 ppm. This suggests a partial rearrangement to the *cis*-isomer. After continuous stirring for several hours, the <sup>13</sup>C NMR spectrum now shows one resonance for the quaternary carbon atom at 190.4 ppm, whereas the single resonance for

(10) Orchin, M.; Schmidt, P. J. *Coord. Chem. Rev.* **1968**, *3*, 345.

(11) Badley, E. M.; Chatt, J.; Richards, R. L.; Sim, G. A. *Chem. Commun.* **1969**, 1322.

**Table 2. Selected Parameters for the Complexes *cis*-[PdCl<sub>2</sub>(L<sup>Allyl</sup>)PEt<sub>3</sub>], **2**, *cis*-[PdCl<sub>2</sub>(L<sup>Allyl</sup>)<sub>2</sub>], **3**, and *trans*-[PdCl<sub>2</sub>(L<sup>Allyl</sup>)<sub>2</sub>], **4**<sup>a</sup>**

<i>cis</i> -[PdCl <sub>2</sub> (L <sup>Allyl</sup> )PEt <sub>3</sub> ], <b>2</b>		<i>cis</i> -[PdCl <sub>2</sub> (L <sup>Allyl</sup> ) <sub>2</sub> ], <b>3</b>			<i>trans</i> -[PdCl <sub>2</sub> (L <sup>Allyl</sup> ) <sub>2</sub> ], <b>4</b>		
parameter	exptl (X-ray)	parameter	exptl (X-ray)	theoretical DFT, LSDA (GGA)	parameter	exptl (X-ray)	theoretical DFT, LSDA (GGA)
<b>Bond Length</b>		<b>Bond Length</b>			<b>Bond Length</b>		
Pd–Cl(2)	2.3636(12)	Pd–C(1)	1.997(13)	1.974 (1.998)	Pd–C(1)	2.032(2)	2.029 (2.041)
Pd–C(1)	1.972(4)	Pd–C(11)	1.993(13)	1.984 (2.005)	Pd–Cl(1)	2.306(1)	2.321 (2.368)
Pd–Cl(1)	2.3685(12)	Pd–Cl(2)	2.342(4)	2.320 (2.389)	C(1)–N(1)	1.323(3)	1.336 (1.339)
Pd–P	2.2524(12)	Pd–Cl(1)	2.365(3)	2.318 (2.384)	C(1)–N(2)	1.323(4)	1.335 (1.337)
C(1)–N(1)	1.328(5)	C(1)–N(1)	1.307(16)	1.346 (1.348)	N(1)–C(2)	1.468(4)	1.457 (1.465)
C(1)–N(2)	1.334(5)	C(1)–N(2)	1.304(16)	1.339 (1.339)	C(2)–C(3)	1.525(5)	1.530 (1.534)
N(1)–C(2)	1.474(6)	N(1)–C(2)	1.471(17)	1.470 (1.467)	C(3)–N(2)	1.468(3)	1.460 (1.465)
C(2)–C(3)	1.474(6)	C(2)–C(3)	1.50(2)	1.534 (1.529)			
C(3)–N(2)	1.474(6)	C(3)–N(2)	1.465(16)	1.465 (1.464)			
<b>Bond Angle</b>		<b>Bond Angle</b>			<b>Bond Angle</b>		
C(1)–Pd–C(2)	178.39(13)	C(1)–Pd–Cl(2)	175.8(4)	173.011 (181.19)	C(1)–Pd–C(1A)	180.0(1)	179.99 (179.99)
P–Pd–Cl(1)	177.71(4)	C(11)–Pd–Cl(1)	173.8(5)	175.31 (180.08)	Cl(1)–Pd–Cl(2)	180.0(1)	179.99 (179.99)
Cl(2)–Pd–Cl(1)	93.79(5)	C(1)–Pd–C(11)	91.2(5)	94.98 (96.64)	C(1)–Pd–Cl(1)	90.7(1)	90.63 (90.28)
Cl(1)–Pd–C(1)	87.00(12)	C(11)–Pd–Cl(2)	86.6(4)	88.15 (84.55)	C(1A)–Pd–Cl(1)	89.3(1)	89.36 (89.71)
Pd–C(1)–N(1)	125.2(3)	Pd–C(1)–N(1)	123.00(12)	123.75 (125.74)	Pd–C(1)–N(1)	125.7(2)	124.87 (125.82)
Pd–C(1)–N(2)	125.4(3)	Pd–C(1)–N(2)	128.5(10)	127.11 (125.63)	Pd–C(1)–N(2)	125.6(2)	126.14 (125.47)
N(1)–C(1)–N(2)	109.4(4)	N(1)–C(1)–N(2)	108.5(12)	108.96 (108.57)	N(1)–C(1)–N(2)	108.86(2)	108.97 (108.70)
<i>E</i> <sub>Total</sub> (kcal mol <sup>-1</sup> )				–4243818.08			–4243810.91
				(–4223158.52)			(–4223164.06)

<sup>a</sup> The calculated data for the optimized geometry for the **3** and **4** are included.

the ring protons becomes in the <sup>1</sup>H NMR spectrum an AB doublet. This can be explained by assuming a *cis* geometry.

The [PdX<sub>2</sub>(PR<sub>3</sub>)<sub>2</sub>] (X = halide) compounds tend to have a *trans* configuration, since the monodentate phosphines produce high steric repulsion. In contrast, despite the poor quality of the data, the structural parameters for **3** (Figure 2) show in accord with other experimental results<sup>12</sup> that the two L<sup>Allyl</sup> ligands are in a *cis* arrangement and that they are orthogonal to the PdCl<sub>2</sub> plane; this latter feature relieves the steric congestion. The average values of the ring dimensions compare favorably with those determined experimentally for the *trans*-[PdCl<sub>2</sub>(L<sup>Allyl</sup>)<sub>2</sub>] complex **4**. The Pd–C bond lengths (1.993(13) and 1.997(13) Å) lie in the range of those reported for other carbene complexes (1.95–2.07 Å).<sup>13–17</sup> In this regard the Pd–Cl bond length is greater than that of complex **4**, reflecting the high *trans* influence of the carbene ligand.

Although some examples of *cis* → *trans* isomerization have been reported,<sup>18</sup> very few cases of *trans* → *cis* rearrangements have been observed.<sup>19–21</sup> Several experimental<sup>22</sup> and theoretical<sup>23</sup> studies have addressed

this isomerization process; in particular, an interesting theoretical study of *cis*-bis(carbene) systems has been reported.<sup>24</sup> However, an assessment of the relative thermodynamic stabilities of the two isomers has not been reported. With the purpose of obtaining a more quantitative description of its structural and energetic features, we have performed theoretical calculations using density functional theory (DFT)<sup>25,26</sup> techniques.

For the molecules *cis*-**3** and *trans*-**4**, calculations were carried out with two different DFT approximations to the exchange–correlation potential: the local spin density approximation (LSDA) and the B3LYP generalized gradient approximation (GGA). The LSDA and GGA calculations were done with the programs DGauss<sup>27</sup> and Gaussian-98,<sup>28</sup> respectively. The main technical feature is that both LSDA and GGA produce accurate geometries, where, for instance, the calculated bond lengths differ by about 0.01–0.05 Å from the experimental values.<sup>29</sup> However, LSDA overestimates signifi-

(23) Albright, T. A.; Burdett, J. K.; Whangbo, M. H. In *Orbital Interactions in Chemistry*; Wiley: New York, 1985; p 304.

(24) Cauchy, D.; Jean, Y.; Eisenstein, O.; Volatron, F. *Organometallics* **1988**, *7*, 829.

(25) Hohenberg, P.; Kohn, W. *Phys. Rev.* **1964**, *136*, B864. Kohn, W.; Sham, L. J. *Phys. Rev.* **1965**, *140*, A1133.

(26) Parr, R. G.; Yang, W. *Density-Functional Theory of Atoms and Molecules*; Oxford University Press: New York, 1989.

(27) Andzelm, J. In *Density Functional Methods in Chemistry*; Labanowski, J.; Andzelm, J., Eds.; Springer: New York, 1991.

(28) Frisch, M. J.; Trucks, G. W.; Schlegel, H. B.; Scuseria, G. E.; Robb, M. A.; Cheeseman, J. R.; Zakrzewski, V. G.; Montgomery, J. A.; Stratmann, R. E.; Burant, J. C.; Dapprich, S.; Millam, J. M.; Daniels, A. D.; Kudin, K. N.; Strain, M. C.; Farkas, O.; Tomasi, J.; Barone, V.; Cossi, M.; Cammi, R.; Mennucci, B.; Pomelli, C.; Adamo, C.; Clifford, S.; Ochterski, J.; Petersson, G. A.; Ayala, P. Y.; Cui, Q.; Morokuma, K.; Malick, D. K.; Rabuck, A. D.; Raghavachari, K.; Foresman, J. B.; Cioslowski, J.; Ortiz, J. V.; Stefanov, B. B.; Liu, G.; Liashenko, A.; Piskorz, P.; Komaromi, I.; Gomperts, R.; Martin, R. L.; Fox, D. J.; Keith, T.; Al-Laham, M. A.; Peng, C. Y.; Nanayakkara, A.; Gonzalez, C.; Challacombe, M.; Gill, P. M. W.; Johnson, B. G.; Chen, W.; Wong, M. W.; Andres, J. L.; Head-Gordon, M.; Replogle, E. S.; Pople, J. A. *GAUSSIAN 98* (Revision A.1); Gaussian Inc.: Pittsburgh, 1998.

(29) Foresman, J. B.; Frisch, A. *Exploring Chemistry with Electronic Structure Methods*, 2nd ed.; Gaussian, Inc.: Pittsburgh, 1993; p 149.

(12) Herrmann, W. A.; Elison, M.; Fisher, J.; Kocher, Ch.; Artus, G. R. *J. Angew. Chem., Int. Ed. Engl.* **1995**, *34*, 2371.

(13) Wilson, R. D.; Kamitori, Y.; Ogoshi, H.; Yoshida, Z.-I.; Ibers, J. A. *J. Organomet. Chem.* **1979**, *173*, 199.

(14) Modinos, A.; Woodward, P. *J. Chem. Soc., Dalton Trans.* **1974**, 2065.

(15) Domiano, P.; Musatti, A.; Ardelli, M.; Predieri, G. *J. Chem. Soc., Dalton Trans.* **1975**, 2165.

(16) Clark, H. C.; Milne, C. R. C.; Pyne, N. C. *J. Am. Chem. Soc.* **1978**, *100*, 1164.

(17) Buttler, W. M.; Enemark, J. H. *Inorg. Chem.* **1971**, *10*, 2416.

(18) Herrmann, W. A.; Fischer, J.; Öfele, K.; Artus, G. R. *J. Organomet. Chem.* **1997**, *530*, 259.

(19) Thomas, R. E.; Orchin, W. M. *J. Am. Chem. Soc.* **1970**, *92*, 1078.

(20) Adden, E. A.; Johnson, N. P.; Rosevear, D. T.; Wilkinson, W. *Chem. Commun.* **1971**, 171.

(21) Çetinkaya, B.; Çetinkaya, E.; Lappert, M. F. *J. Chem. Soc., Dalton Trans.* **1973**, 906.

(22) Redfield, D. A.; Cary, L. W.; Nelson, J. H. *Inorg. Chem.* **1975**, *14*, 50.



cantly the binding energies of transition metal–ligand systems; the errors may be 10–50% or even higher in highly correlated systems.<sup>30,31</sup> The introduction of GGA corrects, at least partially, the LSDA overbinding. However, when compared with the experiment,<sup>30,31</sup> the remaining errors still are big, of about 10–20%.

DFT calculations, of the all-electron type, were carried out for the molecules *cis*-**3** and *trans*-**4**. The geometries were optimized (bond lengths and bond angles were simultaneously refined) by minimizing the norm of the gradient, with a  $10^{-5}$  au threshold. High convergence criteria were used for the total energy, with a tolerance of  $10^{-7}$  au. Table 2 lists some structural parameters together with pertinent comparisons with experimental results. There is excellent agreement between the calculated values and those measured from the crystal structures. In particular, the Pd–C distance was correctly predicted, namely, 2.029 Å, compared to the experimental value, 2.032(2) Å. Furthermore, the arrangement of the ligands around the palladium atom was reproduced, and the coordination of the Cl ligands to the palladium atom is almost exactly the same as that observed in the crystal structure.

Even more interesting than the agreement of the DFT predictions with experimental geometries are the energetics provided by these calculations. Complex **3**, *cis*-isomer, is computed to be more stable, at the LSDA level of theory, than *trans*-isomer **4** by only 7.17 kcal mol<sup>-1</sup> (Table 2), suggesting that the preferred formation of **4** over **3** is kinetically controlled. But the GGA results indicate that *trans*-isomer **4** is slightly more stable, by 5.5 kcal mol<sup>-1</sup>, than the *cis*-isomer. Note that our computed LSDA and GGA values fall in the error bar of DFT calculations. So, these results indicated a quasi-degeneracy for the *cis*- and *trans*-isomers. It is presently not clear if *cis*-isomer **3** is capable of isomerizing to the *trans* isomer. However, an additional electronic factor contributing to the relative stability of complex **3** appears to be the major degree of Pd → C back-donation to the carbene carbon atom. Such back-donation would reduce the electron population in the metal d orbitals and, consequently, the electrostatic repulsion experienced by the *trans*-chlorine atoms. On the other hand, a tetrahedral transition state has been proposed to be the conversion of square planar complexes and its isomerization barrier calculated<sup>32</sup> to be 26 kcal mol<sup>-1</sup>. Using a tetrahedral transition state as a model of the *trans*–*cis* transformation, we have estimated a GGA barrier of 16 kcal mol<sup>-1</sup>. It is to be mentioned that the tetrahedral transition state decays, through geometry optimization, into the *cis*-isomer, confirming the stability of this state.

## Conclusions

In summary, amination **1** has proven to provide an alternative route to metal carbene complexes, when rearrangement reactions are possible in higher yields than in situ reactions.<sup>6,7</sup> Thermal treatment of Pd(II) and Pt(II) complexes of *trans*-[MCl<sub>2</sub>(L<sup>Me</sup>)PEt<sub>3</sub>] leads to a mixture of *cis* and *trans* complexes in thermal equi-

librium,<sup>21</sup> suggesting that the two isomers are of comparable stability. Our calculation gives insight into this behavior: isomers **3** and **4** are indeed of comparable stability, differing in energy by no more than 5.5 kcal mol<sup>-1</sup>.

## Experimental Section

**General Procedures.** All experiments were performed under argon using freshly distilled dry solvents. The following starting materials were prepared and purified according to the literature methods: [C<sub>3</sub>H<sub>5</sub>NCH<sub>2</sub>CH<sub>2</sub>(C<sub>3</sub>H<sub>5</sub>)NC(NMe<sub>2</sub>)H],<sup>33</sup> **1**, [Pd<sub>2</sub>Cl<sub>4</sub>(PEt<sub>3</sub>)<sub>2</sub>],<sup>34</sup> *trans*-[PdCl<sub>2</sub>(L<sup>Allyl</sup>)PEt<sub>3</sub>],<sup>8</sup> *trans*-[PdCl<sub>2</sub>(L<sup>Allyl</sup>)<sub>2</sub>].<sup>8</sup> IR spectra in the 4000–200 cm<sup>-1</sup> range were obtained on a Nicolet Magna 750 FT-IR spectrophotometer as Nujol mulls. The <sup>1</sup>H, <sup>13</sup>C{<sup>1</sup>H}, and <sup>31</sup>P{<sup>1</sup>H} NMR spectra were measured at room temperature on a Varian NOVA 300 spectrometer in CDCl<sub>3</sub>; TMS was used as an internal standard for <sup>1</sup>H NMR spectroscopy (300.2 MHz), and the central peak of CDCl<sub>3</sub> at δ 76.90 was used for <sup>13</sup>C{<sup>1</sup>H} NMR spectroscopy (75.5 MHz). Mass spectra was obtained on a JEOL JMS-SX102A at 70 eV. Melting points were recorded using an electrothermal melting point apparatus and are uncorrected. Elemental analyses were performed by Galbraith Laboratories, Inc., Knoxville, TN.

**Reaction of 1,3-Diallyl-2-dimethylaminoimidazolidine, 1. (a) With Dichlorobis(triethylphosphine)-μ-dichlorodipalladium(II).** A benzene solution of the amination **1** (0.074 g, 0.38 mmol) was added with vigorous stirring to a suspension of the palladium complex (0.098 g, 0.16 mmol) in benzene (25 mL). A light orange solution was formed. The color gradually faded, and a white precipitate was formed. After 1.0 h, this was isolated by filtration and washed with ether to yield *cis*-dichloro(1,3-diallylimidazolidin-2-ylidene)(triethylphosphine)-palladium(II), **2** (0.10 g, 70.12%). Mp: 194–195 °C. Anal. Calcd for C<sub>15</sub>H<sub>29</sub>Cl<sub>2</sub>N<sub>2</sub>PPd: C, 40.4; H, 6.5; N, 6.2. Found: C, 40.7; H, 6.5; N, 6.4. <sup>31</sup>P{<sup>1</sup>H} NMR (δ ppm): 30.0 (s, PEt<sub>3</sub>). <sup>1</sup>H NMR (CDCl<sub>3</sub>, δ ppm): 6.0 (m, 2H, =CH), 5.3 (m, 4H, CH<sub>2</sub>=), 4.6 (m, 4H, RCH<sub>2</sub>N), 3.6 (d, 4H, N(CH<sub>2</sub>)<sub>2</sub>N), 1.2 (two t, 9H, J<sub>CH<sub>3</sub>-CH<sub>2</sub></sub> = 7.6 Hz, J<sub>P-CH<sub>3</sub></sub> = 17.6 Hz), 1.9 (m, 6H, P-CH<sub>2</sub>). <sup>13</sup>C{<sup>1</sup>H} NMR (CDCl<sub>3</sub>, δ ppm): 193.3 (s, C<sub>carbene</sub>), 132.1 (s, =CH), 120.2 (s, CH<sub>2</sub>=), 54.0 (s, RCH<sub>2</sub>N), 48.1 (s, N(CH<sub>2</sub>)<sub>2</sub>N), 8.2 (s, P-CH<sub>3</sub>), 16.8 (d, J<sub>P-CH<sub>2</sub></sub> = 31.9 Hz). IR: 1647.1 ν(CH<sub>2</sub>=CH), 1516.0 ν(CN<sub>2</sub>), 302.9, 284.4 ν(Pd–Cl) cm<sup>-1</sup>. MS (*m/z*): 446.

**(b) With *cis*-Dichloro **2** Complex.** The same procedure as (a) was employed. The *cis*-palladium complex **2** (0.2 g, 0.44 mmol) and amination (0.109 g, 0.56 mmol) gave *cis*-dichlorobis(1,3-diallylimidazolidin-2-ylidene)palladium(II), **3** (0.19 g, 93%). This same complex has been obtained from the rearrangement of *trans*-bis(carbene) complex **4**: *trans* complex **4** was stirred at room temperature in benzene (30 mL). The yellow color of the solution was discharged after 48 h. Upon cooling, colorless crystals of the *cis*-isomer were deposited. The crystals were isolated by filtration and washed with cold benzene. Mp: 140.0 °C (dec). Spectroscopic data for complex **3**. <sup>1</sup>H NMR (CDCl<sub>3</sub>, δ ppm): 5.8 (m, 4H, =CH), 5.2 (m, 8H, CH<sub>2</sub>=), 4.5 (m, 8H, RCH<sub>2</sub>N), 3.5 (d, 8H, N(CH<sub>2</sub>)<sub>2</sub>N). <sup>13</sup>C{<sup>1</sup>H} NMR (CDCl<sub>3</sub>, δ ppm): 190.4 (s, C<sub>carbene</sub>), 132.6 (s, =CH), 119.1 (s, CH<sub>2</sub>=), 53.6 (s, RCH<sub>2</sub>N), 47.8 (s, N(CH<sub>2</sub>)<sub>2</sub>N). IR: 1639.4 ν(CH<sub>2</sub>CH), 1514.1 ν(CN<sub>2</sub>), 402.7, 386.5 ν(Pd–Cl) cm<sup>-1</sup>. MS (*m/s*): 477

**Chloride Replacement. (a) Reaction with Lithium Bromide.** The *cis*-dichloride **2** (0.039 g, 0.088 mmol) was treated with an excess of LiBr (ca. 50-fold) in acetone at room temperature for 24 h. The solvent was removed in a vacuum, and the residue was washed with water (3 × 5 mL) and then recrystallized from CHCl<sub>3</sub> to yield *cis*-dibromo(1,3-diallylimidazolidin-2-ylidene)(triethylphosphine)palladium(II), **5** (0.033

(30) Fournier, R. *J. Chem. Phys.* **1993**, *99*, 1801.

(31) Castro, M.; Salahub, D. R.; Fournier, R. *J. Chem. Phys.* **1994**, *100*, 8233.

(32) Halevi, E. A.; Knorr, R. *Angew. Chem. Suppl.* **1982**, 622.

(33) Çetinkaya, B.; Çetinkaya, E.; Chamizo, J. A.; Hitchcock, P. B.; Jasim, H. A.; Küçükbay, H.; Lappert, M. F. *J. Chem. Soc., Perkin Trans.* **1998**, *1*, 2047.

(34) Chatt, J.; Venanzi, L. M. *J. Chem. Soc.* **1957**, 2351.

g, 70.1%). Mp: 198.0 °C (dec).  $^{31}\text{P}\{^1\text{H}\}$  NMR ( $\delta$  ppm): 29.0 (s,  $\text{PEt}_3$ ).  $^1\text{H}$  NMR ( $\text{CDCl}_3$ ,  $\delta$  ppm): 5.9 (m, 2H, =CH), 5.2 (m, 4H,  $\text{CH}_2=$ ), 4.4 (m, 4H,  $\text{RCH}_2\text{N}$ ), 3.5 (d, 4H,  $\text{N}(\text{CH}_2)_2\text{N}$ ), 1.1 (two t, 9H,  $J_{\text{CH}_3-\text{CH}_2} = 7.5$  Hz,  $J_{\text{P}-\text{CH}_3} = 17.3$  Hz), 1.8 (m, 6H, P- $\text{CH}_2$ ).  $^{13}\text{C}\{^1\text{H}\}$  NMR ( $\text{CDCl}_3$ ,  $\delta$  ppm): 193.0 (s,  $\text{C}_{\text{carbene}}$ ), 131.9 (s, =CH), 120.1 (s,  $\text{CH}_2=$ ), 53.8 (s,  $\text{RCH}_2\text{N}$ ), 48.1 (s,  $\text{N}(\text{CH}_2)_2\text{N}$ ), 8.3 (s, P- $\text{CH}_3$ ), 17.3 (d,  $J_{\text{P}-\text{CH}_2} = 31.1$  Hz). IR: 1647.1  $\nu(\text{CH}_2=\text{CH})$ , 1523.1  $\nu(\text{CN}_2)$ , 270.1, 230.6  $\nu(\text{Pd}-\text{Br})$   $\text{cm}^{-1}$ . MS ( $m/z$ ): 535.

**(b) Reaction with Sodium Iodide.** *cis*-Diiodo(1,3-dialylimidazolidin-2-ylidene)(triethylphosphine)palladium(II), **6**, was prepared in the same manner as the bromide analogue from NaI (0.045 g, 81.3%). Mp: 263.0 °C.  $^{31}\text{P}\{^1\text{H}\}$  NMR ( $\delta$  ppm): 24.0 (s,  $\text{PEt}_3$ ).  $^1\text{H}$  NMR ( $\text{CDCl}_3$ ,  $\delta$  ppm): 5.9 (m, 2H, =CH), 5.2 (m, 4H,  $\text{CH}_2=$ ), 4.3 (m, 4H,  $\text{RCH}_2\text{N}$ ), 3.5 (d, 4H,  $\text{N}(\text{CH}_2)_2\text{N}$ ), 1.1 (two t, 9H,  $J_{\text{CH}_3-\text{CH}_2} = 7.8$  Hz,  $J_{\text{P}-\text{CH}_3} = 17.4$  Hz), 1.9 (m, 6H, P- $\text{CH}_2$ ).  $^{13}\text{C}\{^1\text{H}\}$  NMR ( $\text{CDCl}_3$ ,  $\delta$  ppm): 194.7 (s,  $\text{C}_{\text{carbene}}$ ), 131.6 (s, =CH), 120.2 (s,  $\text{CH}_2=$ ), 53.9 (s,  $\text{RCH}_2\text{N}$ ), 48.3 (s,  $\text{N}(\text{CH}_2)_2\text{N}$ ), 8.3 (s, P- $\text{CH}_3$ ), 18.0 (d,  $J_{\text{P}-\text{CH}_2} = 31.1$  Hz). IR: 1643.3  $\nu(\text{CH}_2=\text{CH})$ , 1517.9  $\nu(\text{CN}_2)$ , 189.2  $\nu(\text{Pd}-\text{I})$   $\text{cm}^{-1}$ . MS ( $m/z$ ): 628.

**Crystal Structure Determinations of 2 and 3.** A summary of the crystal data is presented in Table 1. The diffraction data were collected on a Siemens P4/PC diffractometer using graphite monochromatized Mo  $\text{K}\alpha$  radiation, with  $\theta/2\theta$  and  $\omega$  scan modes for **2** and **3**, respectively, at variable scan speed, in the largest  $2\theta$  range possible. Because of the poor quality of **3**, data collection was limited to  $2\theta = 48^\circ$ . An absorption correction was applied using  $\psi$  scans. Subsequent computations were performed using the SHELX97 package.<sup>35</sup> The poor refinement obtained for **3** is mainly due to data ( $R_{\text{int}} = 9.00\%$ ) and to disordered water molecules. Finally, for both structures H atoms were placed in idealized positions (except for  $\text{H}_2\text{O}$  molecules in **3**) and refined using a riding model with fixed isotropic  $U$ . All non-H atoms were refined anisotropically using in the last cycles a convenient weighting scheme. Selected bond distances and angles are listed in Table 2.

**Computational Method.** The density functional calculations reported here are based on the Kohn and Sham approach to density functional theory (DFT).<sup>25,26</sup> Two different implementations of DFT were used: DGauss<sup>27</sup> and Gaussian-98.<sup>28</sup> Both programs incorporate the local spin density approximation (LSDA) and the generalized gradient approximation (GGA).

In DGauss the local spin density approximation (LSDA) was included as in Vosko et al.<sup>36</sup> Orbital basis sets of DZVP2

quality ((63321/5211\*/41+) for Pd, (721/51/1\*) for N and C, and (41/1\*) for H), optimized explicitly for DFT calculations, were used.<sup>37</sup> Additional auxiliary bases of Gaussian-type orbitals were employed to describe the charge density (CD) and the XC potential.<sup>38,39</sup> A tight grid was used (this is a very fine grid which allows accurate determination of gradients or atomic forces yielding structural parameters of high quality). Visualization techniques, as implemented in UniChem,<sup>40</sup> were used for the visualization of the calculated molecular structures, molecular orbitals, and electronic densities. UniChem also provides a platform for the performance of the calculations, which were done on a Cray-YMP4/464 supercomputer.

In Gaussian-98 the generalized gradient approximation (GGA) was employed for the treatment of the exchange–correlation (XC). The B3LYP<sup>41,42</sup> hybrid scheme was used, implicating the combination of the Becke exchange functional with the Lee–Yang–Parr correlation functional. B3 indicates a three fitted parameter functional where a portion of the exchange contribution has been calculated in the same fashion as in the Hartree–Fock (HF) procedure, but using the Kohn–Sham (KS) noninteracting wave function instead of the HF one. The 3-21G\* basis set was employed for all atoms.

Atomic coordinates and other crystallographic data have been deposited with the Cambridge Crystallographic Data Center.

**Acknowledgment.** Financial support provided by CONACYT, Mexico, under Project 34845-E, and from DGAPA-UNAM under project IN-101901 as well as the access to the supercomputer Cray-YMP/464, where the calculations were done, is greatly acknowledged. We also wish to thank María de Jesús Zuñiga, Alfonso T. García, Andrés Cisneros, Dr. Julián Cruz, and Dr. Juventino J. García.

**Supporting Information Available:** This material is available free of charge via the Internet at <http://pubs.acs.org>.

OM020205B

(37) Godbout, N.; Salahub, D. R.; Andzelm, J.; Wimmer, E. *Can. J. Chem.* **1992**, *70*, 560.

(38) St-Amant, A.; Salahub, D. R. *Chem. Phys. Lett.* **1990**, *169*, 387.

(39) Salahub, D. R.; Fournier, R.; Mlynarsky, P.; Papai, I.; St-Amant, A.; Ushio, J. In *Density Functional Methods in Chemistry*; Labanowski, J., Andzelm, J., Eds.; Springer: New York, 1991.

(40) Dixon, D. A.; Fitzgerald, B.; Raeuchle, T. *Visualization Approaches in Quantum Chemistry Using Unichem*. In *Data Visualization in Molecular Science*; Bowie, J. E., Ed.; Addison-Wesley: New York, 1995.

(41) Becke, A. D. *J. Chem. Phys.* **1993**, *98*, 5648.

(42) Lee, C.; Yang, W.; Parr, R. G. *Phys. Rev.* **1988**, *B37*, 785.

(35) Sheldrick, G. M. *SHELX97, Users Manual*; University of Göttingen: Germany, 1997.

(36) Vosko, S. H.; Wilk, L.; Nusair, M. *Can. J. Phys.* **1980**, *58*, 1200.